Measurement of Bromide Ion Affinities for the Air/Water and Dodecanol/Water Interfaces at Molar Concentrations by UV Second Harmonic Generation Spectroscopy

Robert M. Onorato,[†] Dale E. Otten,[†] and Richard J. Saykally*[,†,‡]

Department of Chemistry, University of California, Berkeley, California 94720, and Chemical Sciences Division, Lawrence Berkeley National Laboratory, California 94720

Received: April 16, 2010; Revised Manuscript Received: June 8, 2010

Recent experimental and theoretical work has demonstrated that certain anions can exhibit enhanced concentrations at aqueous interfaces and that the adsorption of bromide is particularly important for chemical reactions on atmospheric aerosols, including the depletion of ozone. UV second harmonic generation resonant with the bromide charge-transfer-to-solvent band and a Langmuir adsorption model are used to determine the affinity of bromide for both the air/water and dodecanol/water interfaces. The Gibbs free energy of adsorption for the former is determined to be −1.4 kJ/mol with a lower 90% confidence limit of −4.1 kJ/mol. For the dodecanol/water interface the data are best fit with a Gibbs free energy of +8 kJ/mol with an estimated lower limit of −4 kJ/mol.

I. Introduction

The adsorption of monovalent inorganic ions to interfaces formed by aqueous solutions with air, hydrocarbons, surfactants, and proteins is a phenomenon of central interest to broad areas of science.[1,2] For example, halides at the interfaces of aqueous aerosols appear to play an important role in atmospheric chemistry.[3−5] In particular, interfacially adsorbed bromide appears to be actively involved in tropospheric ozone depletion. The rate of reaction of interfacial bromide with ozone is at least comparable to and may be much greater than the corresponding rate in the bulk.[6] Measurements of molecular bromine, a product of this reaction, correlate with ozone depletion in the Arctic[7−9] and at midlatitudes.[10−15] Moreover, the adsorption of aqueous ions to hydrophobic and hydrophilic groups of biomolecules affects many biological processes. Hofmeister famously sequenced a number of salts in terms of how effectively they solubilize egg white protein,[16] and an ion is labeled as kosmotropic when it increases protein aggregation and chaotropic when it increases protein solubility in aqueous solutions. It is generally agreed that Hofmeister effects are caused by ion−protein interactions,[17−19] but a complete description of the mechanism remains elusive.

Recent work has firmly established the existence of enhanced concentrations of specific ions at the air/water interface.[20−23] Image charge repulsion, an electrostatic force driving ions away from the interface, has long been invoked to explain surface tension results indicating that the interface is largely devoid of inorganic ions.[24] Although it is now clear that this description of the interface is incorrect for many ions, this electrostatic force is still an important component of a mechanistic explanation. Molecular dynamics (MD) simulations have suggested that large anion polarizability leads to surface adsorption,[23] but experimentally the two properties do not appear to be entirely correlated,[25] A "law of matching water affinities" has been suggested, wherein ions of similar hydration strength tend to bind together as contact ion pairs.[26] MD simulations have shown a tendency for weakly solvated anions to adsorb to hydrophobic regions, while smaller, strongly solvated anions prefer to adsorb to a positive charge, implying that multiple adsorption mechanisms are involved in ion−protein interactions. Another recent MD study finds that when the surface plane is allowed to distort, an energy minimum can exist for an ion at a polar liquid/vapor interface, originating from a competition between strong and opposing electrostatic and entropic forces.[27] This theory demonstrates that the presence and magnitude of the energy minimum is strongly dependent on the size and charge of the ion, but the near-cancellation of the driving forces makes it difficult to use simulations to reliably predict details of specific ion adsorption.

While the adsorption mechanism is not yet clearly understood, numerous experimental methods have been used to assess ion adsorption to aqueous interfaces. Surface tension measurements have quantified relative affinities of a large selection of ions at the air/water interface.[28,29] Electrospray ionization mass spectrometry was used to assess trends in ionic properties of ions that were ejected from water droplets.[25] A depth profile of relative halide concentration has been measured using X-ray photoelectron spectroscopy (XPS) by varying the photoelectron kinetic energy, finding that the concentration of bromide is enhanced at the air/water interface while chloride is not.[22,30] XPS has also demonstrated that the iodide concentration is enhanced at the air/water interface but that the effect is suppressed at the butanol/water interface.[22,31]

Second-order nonlinear spectroscopy studies comprise a large subset of experimental work at aqueous interfaces, as it is inherently sensitive to broken inversion symmetry at both the macroscopic and microscopic scales. Vibrational sum frequency generation (VSFG) experiments probing the −OH stretching region at the air/water interface have indicated enhanced surface concentrations of bromide and iodide,[20] but recently the development of phase-sensitive VSFG has called the interpretation of previous VSFG experiments into question.[32,33] Phase-sensitive VSFG has been used to characterize the interface of basic and acidic solutions, as well as that of sodium iodide.[34] VSFG has also been used to directly measure the vibrational spectrum of thiocyanide at an air/water interface.[35,36] A Hofmeis-

* To whom correspondence should be addressed, saykally@berkeley.edu.
† University of California, Berkeley.
‡ Chemical Sciences Division, Lawrence Berkeley National Laboratory.

10.1021/jp103454r

ter-like series was established using VSFG for ion adsorption to a macromolecule/water interface.[37] Nonresonant second harmonic generation (SHG) has been used to postulate that the interfacial thickness, the depth of broken inversion symmetry, increases linearly with salt concentration.[38] The presence of ions at the air/water[21,23,39−44] and alcohol/water[45] interfaces has been directly confirmed via resonant SHG.

In this paper the adsorption of the weakly chaotropic bromide anion to both the air/water interface and an alcohol/water interface is addressed using UV SHG. Like VSFG, SHG, is a second-order nonlinear process that is interface specific due to symmetry considerations. The charge-transfer-to-solvent (CTTS) band of the anion, located deep in the UV, is utilized as a two-photon resonance both to enhance the SHG signal and to selectively probe the anion. A modified Langmuir adsorption model is used to determine the Gibbs free energy of ion adsorption to the interface, and these interfacial affinities are put into context by comparing with other relevant studies.

II. Methods

A. Experimental Details. All glassware was cleaned using Nochromix dissolved in concentrated sulfuric acid and rinsed with 18.2 MΩ water (Millipore Milli-Q A10). Solutions were made with 18.2 MΩ water and NaBr (Sigma-Aldrich, >99.0%) which was baked in a tube furnace under nitrogen at 500 °C for 8 h. NaBr used without further purification yielded different results than baked NaBr, which is likely due to organic contaminants.[38] Some solutions were also filtered using a polyvinylidene fluoride filter (Millipore GVWP01300) that was thoroughly rinsed with water prior to use and housed in an all-glass filter assembly; these solutions behaved similarly to those that were not filtered. The alcohol monolayer was prepared on the solution surface by floating a 1-dodecanol (Sigma-Aldrich, 98%) crystal on the solution surface, as described by Casson et al.[46] All samples were prepared and measured at room temperature (18 ± 1 °C).

The laser system has been described in detail previously.[39] Briefly, a regenerative amplifier (Spectra-Physics Spitfire, 1 kHz, 100 fs) seeded by a home-built Ti:sapphire oscillator is used to pump an optical parametric amplifier (OPA, Quantronix TOPAS). The tunable output of the OPA is used as the fundamental beam. The fundamental intensity is continuously modulated by a motorized variable neutral density filter. Less than 10% of the modulated fundamental is directed to a photodiode as a reference pulse energy measurement. The p-polarized fundamental is focused onto the sample surface at an angle of incidence of 60° relative to the surface normal. The pulse energy density at the interface is less than 0.3 $J \cdot cm^{-2}$ per pulse. The p-polarized SHG light is collected in the reflection geometry and separated from the fundamental with a series of dichroic mirrors and a monochromator (PI Acton, Spectra Pro SP-2155) before being detected by a solar-blind PMT (Hammamatsu, R7154PHA). The observed signal intensities are on the order of 0.01 photons per pulse.

As SHG is a second-order process, the signal intensity is proportional to the square of the fundamental intensity

$$I_{SHG} = |\chi^{(2)}_{effective}|^2 I^2_{fundamental} \quad (1)$$

where $\chi^{(2)}_{effective}$ is the observed second-order nonlinear susceptibility of the system. The reference pulse energy (R) is binned into groups of $R^2 \pm \Delta$, and the number of pulses where zero photons are detected, $N^{k=0}_{pulses}$, is counted. Poisson statistics are assumed for the distribution of SHG photons detected for each pulse, and the average number of photons for a given $R^2 \pm \Delta$ bin can be evaluated as

$$\langle k \rangle = -\ln\left[\frac{N^{k=0}_{pulses}}{N^{total}_{pulses}}\right]_{R^2 \pm \Delta} \quad (2)$$

Plotting this value versus R^2 provides a linear relationship. The slope of the resulting line, determined by a variance-weighted least-squares fit, is taken as the system response constant, proportional to $|\chi^{(2)}_{effective}|^2$. This also provides an inherent confirmation that the SHG signal exhibits the correct second-order power dependence.

B. Surface Adsorption Model. In order to determine thermodynamic quantities from the SHG signal of an aqueous solution interface, a modified Langmuir adsorption model is used. The model used here has been described in detail elsewhere[39,42,45] and an overview is given here. The solution is partitioned into interfacial and bulk regions and is assumed to obey the equilibrium expression

$$S_S + N_B \rightleftharpoons S_B + N_S \quad (3)$$

S_i is the solvent species and N_i is the solute species, while the subscripts $i = B$ and S indicate that the species resides in the bulk and surface partitions, respectively.

The effective nonlinear susceptibility can be separated into the solvent and the solute contributions, each with complex phase, and is parametrized as

$$|\chi^{(2)}_{effective}|^2 = |A + (B + iC)N_S|^2 \quad (4)$$

where the relative phase of the response of the neat solvent, A, is defined such it is entirely real. The molecular response parameters of the solute species, B and C, can grow large when in resonance with the CTTS band. This effective molecular response is governed by the effective hyperpolarizability, a third rank tensor averaged over molecular orientations.

The number density of surface solute species can be written in terms of the bulk solute concentration

$$N_S = \frac{N^{max}_S [N_B]}{[N_B] + [H_2O]/K} \quad (5)$$

Here N^{max}_S is the number of surface sites and $K = \exp[-\Delta G_{ads}/RT]$. ΔG_{ads} is the Gibbs free energy change of replacing an interfacial solvent species with a solute species. If the concentration dependence of the SHG signal is measured, this free energy can be determined by a fit of parameters A, B, and C.

III. The Air/Water Interface

The bromide CTTS absorption maximum in the bulk is centered near 200 nm.[47] The SHG signal is plotted as a function of bulk sodium bromide concentration in Figure 1a for SHG wavelengths of 193 and 265 nm for the air/water interface. The SHG response is normalized such that the response of neat water is unity. Note that the concentration range spans from 6 mM to 7 M concentrations and that at both 193 and 265 nm the response at 6 mM is less than that of neat water, indicative of destructive interference between the water response and the bromide

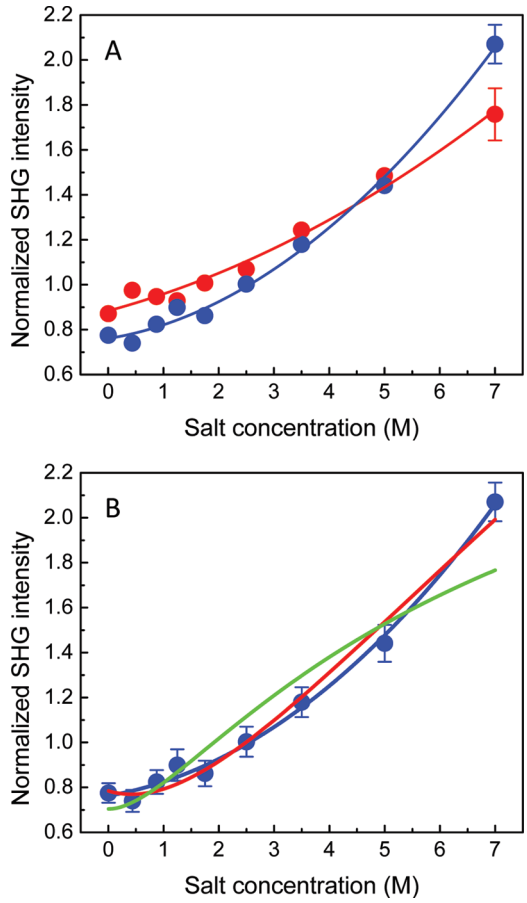

Figure 1. (a) The SHG intensity (blue circle,193 nm and red circle 265 nm) of bromide at the air/water interface normalized to the neat water response as a function of concentration. The lines are the Langmuir isotherm fit to the data. The concentration ranges from 6 mM to 7 M. (b) A comparison of Langmuir isotherm fits to the data (only blue circle 193 nm is pictured) with the free energy of adsorption unconstrained, $\Delta G_{ads} = -1.4$ kJ/mol (blue line), and constrained to values of −4 (red line) and −7 kJ/mol (green line). The −4 kJ/mol fit approximates the data, but the data are not well-represented by the −7 kJ/mol fit.

response at low concentrations (discussed in a future publication). The observed SHG signal is weak relative to a similar ion, iodide; the maximum SHG response of bromide is just twice that of water, whereas for iodide it is 12 times the water response.

A valuable comparison is a nonresonant SHG study by Wang et al.[38] For bromide, chloride, and fluoride they find that the nonresonant signal (SHG = 400 nm) increases linearly with salt concentration, ascribing this to thickening of the interfacial region. The 265 nm data presented here can be fit quite reasonably with a linear model, indicating that this wavelength is nonresonant. However, the 193 nm data do not fit to a linear model; the data are clearly superlinear. We thus conclude that the 193 nm data exhibit a weak resonant enhancement.

The CTTS band of surface bromide anions could be shifted from its known bulk value,[42,48] explaining the weakness of the SHG response at 193 nm. Previous SHG studies at the air/water interface found a small red shift of the surface CTTS band relative to the bulk spectrum,[42] which would indicate a shift away from 193 nm for bromide. However, the SHG response of 7 M (nearly saturated) NaBr was measured at 205 and 210 nm, and both were found to be between the response at 193 and 265 nm (see Table 1). Therefore, it is unlikely that such a shift in the CTTS band is the cause of the weakness of the observed SHG signal.

TABLE 1: SHG Response of the Air/Water Interface of a 7 M Sodium Bromide Solution

wavelength (nm)	normalized SHG response
193	2.07
205	1.84
210	1.84
265	1.76

The strength of the effective hyperpolarizability may also explain the weak bromide response. Bromide, being a smaller and less polarizable ion than iodide, will have a smaller effective hyperpolarizability and thus a weaker SHG response. Measurements of the hyper-Rayleigh scattering (HRS) of a 5 M aqueous sodium bromide solution have indicated that the magnitude of the bromide hyperpolarizability is relatively small, supporting the suggestion that the weak response may simply be due to a relatively weak chromophore.[38] For comparison, the SHG responses of both bromide and iodide are weak relative to thiocyanide ($SHG_{max} \approx 200$ times water). As thiocyanide exhibits broken inversion symmetry on the molecular scale, it has a much larger effective hyperpolarizability than the spherical halides. The relatively weak effective hyperpolarizability of bromide in comparison to iodide may be further exasperated by the solvation structures of these ions at the interface. MD simulations show that bromide ions are less exposed, or better solvated, at the interface than iodide.[49,50] In such a case we can envision that the symmetry of the more-desolvated iodide ion will be broken more severely than that of the bromide, even if the molecular response would otherwise be equal. Therefore, the interfacial structure may enhance the response of iodide more than that of bromide without any net difference in number density.

Finally, the number of ions at the interface may explain the weaker SHG signal of bromide. For the molar concentration regime the Langmuir isotherm fit to the bromide data gives an equilibrium constant, $K = 1.8 \pm 2$, corresponding to a free energy of −1.4 kJ/mol. However, discussing the associated error in the latter is problematic since a negative equilibrium constant is nonphysical. Therefore, the positive limit for the free energy cannot be determined from these data. The inability to determine a positive limit is a manifestation of the simple model used and has been discussed previously.[43] The negative limit of the free energy can be calculated, however, yielding a 90% confidence limit of $\Delta G_{ads} \geq -4.1$ kJ/mol. Figure 1b shows the Langmuir isotherm fits at 193 nm when the free energy is constrained to −4 and −7 kJ/mol in comparison to the unconstrained fit and the experimental data. The −4 kJ/mol fit appears to be reasonable, considering the data and the associated error; however, the −7 kJ/mol fit does not match the experiment. This agrees well with the above calculated lower limit for the free energy. The free energy of iodide adsorption was previously determined to be consistent with both −3.3 and 0 kJ/mol, although no finite limits were given.[42] On the basis of these results, the relative number of surface bromide and iodide ions cannot be determined.

Previously, the adsorption of thiocyanide,[23] nitrate,[43] iodide,[42] and hydroxide[44] to the air/water interface were also studied by UV SHG for concentrations in the molar regime. The reported lower limit, best fit, and upper limit of the Gibbs free energy are reported in Table 2. On the basis of these results, it is not possible to order the free energies of these ions beyond noting that thiocyanide is the most strongly adsorbed. Compiling the

TABLE 2: Anion Affinities for the Air/Water Interface Determined by SHG

anion	lower limit	ΔG_{ads} (kJ/mol)	upper limit	reference
SCN^-	−7.6	−7.5	−7.4	23
I^-	−3.3[a]	NA	0[a]	42
NO_3^-	−2	15	NA	43
Br^-	−4.1	−1.4	NA	this study
OH^-	−4	NA	NA	44

[a] The lower and upper limits are not statistically determined in this case. The data were said to be in agreement with either energy, and the actual limits are likely larger.

results from other experimental techniques by Pegram and Record,[29] Cheng et al.,[25] and Ghosal et al.[22] yields the following sequence in order of decreasing interfacial affinity: $SCN^- > I^- > NO_3^- > Br^- > OH^-$.

IV. The Dodecanol/Water Interface

The structure of the dodecanol/water interface has been well characterized. The dodecanol molecules are tightly packed with a surface area of 20 Å/molecule[51] while the aliphatic chains stand nearly vertical.[52,53] This surface structure is largely unaffected by the presence of salt.[51] This leaves the hydroxyl terminus free to interact with the solvent via hydrogen bonding or to explicitly contribute to the solvation shell of an anion approaching the interfacial plane. VSFG demonstrated that there is little evidence of non-hydrogen-bonded −OH groups at the alcohol/water interface.[54]

The SHG response of bromide at the dodecanol/water interface is out of phase with the water/dodecanol response, and thus initially decreases as a function of increasing concentration (see Figure 2a). The ratio of the nonresonant SHG response at the dodecanol/water interface and the air/water interface is 3.2 to 1 at both 193 and 265 nm, demonstrating a significantly stronger resonant enhancement of the SHG signal at the dodecanol/water interface than at the air/water interface. Calculating the resonant enhancement as

$$\delta = \frac{\Delta SHG_{193}}{\Delta SHG_{265}} \quad (6)$$

where ΔSHG is the change in SHG from the lowest to highest concentration and the enhancement factor is nearly 6 at the dodecanol/water interface but only 1.5 at the air/water interface.

There are two potential explanations for the increased resonant response. First, different interfacial structures may yield different effective hyperpolarizabilities, as discussed earlier. However, in this case the contribution of the hydroxyl group of dodecanol to the solvation shell of interfacial bromide may present a different local environment to the ion than at the air/water interface. If the spherical shape of bromide is deformed more on average at the dodecanol/water interface than at the air/water interface, the correspondingly larger effective hyperpolarizability could explain the stronger resonant response.

The second possibility is that there are simply more bromide ions at the interface. This would indicate either that bromide is adsorbed more strongly, that there are more surface sites at the dodecanol/water interface, or some combination of these phenomena. The model used here does not explicitly establish the number of surface sites, so only the relative affinity of bromide for the two interfaces can be directly compared.

The Langmuir isotherm fit shown in Figure 2a yields a free energy of +8 kJ/mol. The error is large, and constraining the free energy to the lower limit of the error does not reproduce the shape of the data. Instead, a lower limit is estimated by plotting isotherms fitting the data with the free energy constrained to a specific value and judging the fidelity to the data. Similar to the air/water interface data, an upper limit cannot be determined. Decreasing the free energy near −4 kJ/mol, the isotherms progress from closely approximating the data to no longer reproducing the shape of the data. Isotherms are plotted for representative free energies in Figure 2b. Therefore, we estimate a lower limit of −4 kJ/mol to the free energy. Similar to its behavior at the air/water interface, bromide does not have a strong affinity for the dodecanol/water interface at molar bulk concentrations.

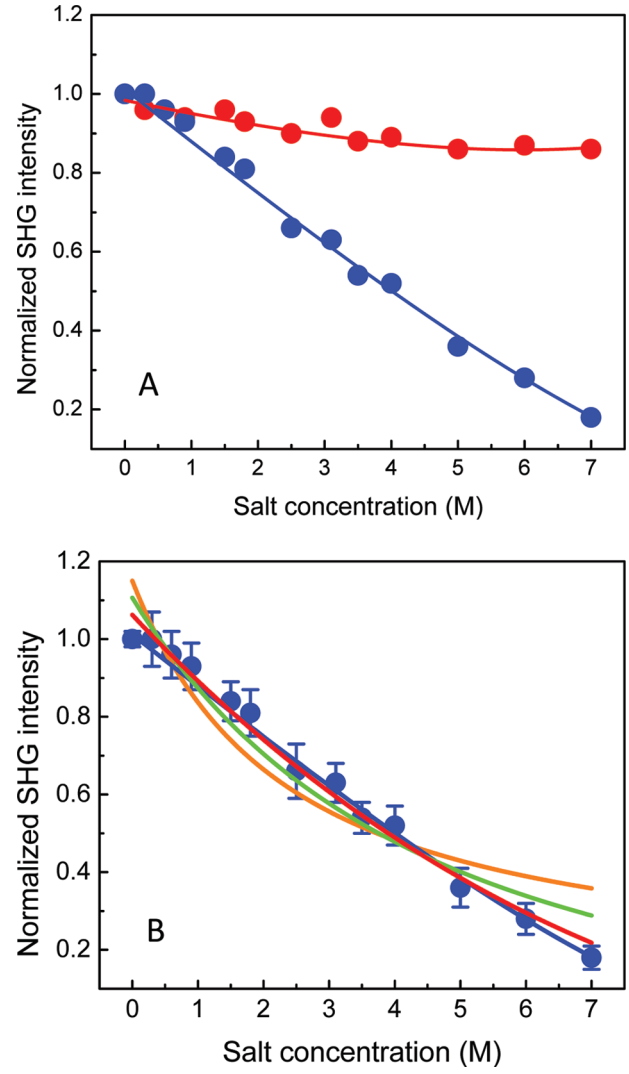

Figure 2. (a) The SHG intensity (blue circle 193 nm and red circle 265 nm) of bromide at the dodecanol/water interface normalized to the water/dodecanol response as a function of concentration. The lines are the Langmuir isotherm fit to the data. The concentration ranges from 0 to 7 M. (b) A comparison of Langmuir isotherm fits to the data (only blue circle 193 nm is pictured) with the free energy of adsorption unconstrained, $\Delta G_{ads} = 8$ kJ/mol (blue line), and constrained to values of −2 (red line), −4 (green line), and −7 kJ/mol (orange line). The −2 kJ/mol fit reasonably approximates the data, but the data are not well represented by the −4 or −10 kJ/mol fits.

On the basis of the results presented here, it cannot be concluded whether the bromide interfacial affinity is greater for the air/water interface or the dodecanol/water interface. Considering the forces that determine the extent of surface adsorption, it is not clear to which interface stronger adsorption would

be predicted. One of the major forces driving ions to the interface is the entropy gain due to hydrophobic exclusion of the ion. At the dodecanol/water interface this force is weaker because even ions at the interface disrupt the hydrogen bonding network. However, the electrostatic force associated with image charge repulsion, the major force inhibiting ion adsorption, should also be weaker at the dodecanol/water interface, since the dispersion forces of the alkyl chains can screen the ionic charges from their images much better than the low-dielectric vapor. A recent MD simulation addressing ion adsorption at the air/water interface emphasized the importance of interfacial flexibility on interfacial ion adsorption.[27] This is particularly interesting, considering that the dodecanol/water interface will be considerably less easily deformed than the air/water interface.

The adsorption of thiocyanide to both the air/water[23] and dodecanol/water[45] interfaces can also be considered. Thiocyanide adsorbed to both interfaces more strongly than bromide, −7.5 kJ/mol in the case of air/water and −6.7 kJ/mol in the case of dodecanol/water. Similar to bromide, the difference in the affinity of thiocyanide to the air/water and dodecanol/water interfaces is within the error of the measurement. In contrast to the bromide results, the maximum thiocyanide SHG response is an order of magnitude weaker at the dodecanol/water interface (20 times water) than at the air/water interface (200 times water). The effective hyperpolarizability is strongly dependent on the orientation of the ions at the interface. As thiocyanide is not spherically symmetric, it is likely that the average ion orientation is different at aqueous interfaces with vapor and dodecanol. Since the strength of adsorption is similar for thiocyanide at the air/water and dodecanol/water interfaces, the change in average ion orientation and possibly fewer surface sites must account for the weaker SHG signal at the dodecanol/water interface.

Another experimental technique has also been used to compare ion interfacial affinities to air/water and alcohol/water interfaces. XPS depth profiling of potassium iodide indicates a weaker concentration enhancement of iodide at the air/butanol/water interface than at the air/water interface.[22,31] The dodecanol/water interface is much more rigid than the butanol/water interface, generally presenting the hydrophilic −OH to the liquid. Butanol exposes a much greater proportion of hydrophobic sites to water at the interface, so the experiments are not directly comparable. It would be interesting to compare a SHG study of iodide at the dodecanol/water interface to these XPS results and to compare an XPS study of bromide and thiocyanide to the SHG results.

V. Conclusions

The structure of a liquid interface exerts a strong effect on the observed SHG response of adsorbed anions. Bromide exhibits only a very weak resonant response at the air/water interface, but the response is significantly stronger at the alcohol/water interface. Both the number of ions at the interface and their effective hyperpolarizability are expected to contribute to this effect, but more detailed conclusions cannot be made.

At molar concentrations the bromide anion shows at most a weak affinity for both the air/water and alcohol/water interfaces at molar concentrations. Using a modified Langmuir adsorption model, the lower 90% confidence limit of the Gibbs free energy of adsorption is −4.1 kJ/mol at the air/water interface with a best fit of −1.4 kJ/mol. Similarly, at the dodecanol/water interface the lower limit is near −4 kJ/mol, but with a best fit of +8 kJ/mol. No upper limit to the free energy could be determined for either interface. Measuring the full CTTS spectrum via SHG would allow for a more detailed understanding of ion adsorption. However, under the current experimental arrangement acquiring a detailed spectrum for a range of concentrations is prohibitively time-consuming. Regardless of its actual surface affinity, bromide ions are clearly present in detectable numbers at both the air/water and surfactant/water interfaces, consistent with the interpretation of recent atmospheric measurements and laboratory kinetic studies.

Acknowledgment. The initial stages of this work were partially supported by the Experimental Physical Chemistry Division of the National Science Foundation (Grant # CHE-0650950).

References and Notes

(1) Petersen, P. B.; Saykally, R. J. *Annu. Rev. Phys. Chem.* **2006**, *57*, 333.
(2) Jungwirth, P.; Winter, B. *Annu. Rev. Phys. Chem.* **2008**, *59*, 343.
(3) Hu, J. H.; Shi, Q.; Davidovits, P.; Worsnop, D. R.; Zahniser, M. S.; Kolb, C. E. *J. Phys. Chem.* **1995**, *99*, 8768.
(4) Knipping, E. M.; Lakin, M. J.; Foster, K. L.; Jungwirth, P.; Tobias, D. J.; Gerber, R. B.; Dabdub, D.; Finlayson-Pitts, B. J. *Science* **2000**, *288*, 301.
(5) Garrett, B. C. *Science* **2004**, *303*, 1146.
(6) Hunt, S. W.; Roeselova, M.; Wang, W.; Wingen, L. M.; Knipping, E. M.; Tobias, D. J.; Dabdub, D.; Finlayson-Pitts, B. J. *J. Phys. Chem. A* **2004**, *108*, 11559.
(7) Impey, G. A.; Shepson, P. B.; Hastie, D. R.; Barrie, L. A.; Anlauf, K. G. *J. Geophys. Res., [Atmos.]* **1997**, *102*, 16005.
(8) Foster, K. L.; Plastridge, R. A.; Bottenheim, J. W.; Shepson, P. B.; Finlayson-Pitts, B. J.; Spicer, C. W. *Science* **2001**, *291*, 471.
(9) Spicer, C. W.; Plastridge, R. A.; Foster, K. L.; Finlayson-Pitts, B. J.; Bottenheim, J. W.; Grannas, A. M.; Shepson, P. B. *Atmos. Environ.* **2002**, *36*, 2721.
(10) Dickerson, R. R.; Rhoads, K. P.; Carsey, T. P.; Oltmans, S. J.; Burrows, J. P.; Crutzen, P. J. *J. Geophys. Res., [Atmos.]* **1999**, *104*, 21385.
(11) Nagao, I.; Matsumoto, K.; Tanaka, H. *Geophys. Res. Lett.* **1999**, *26*, 3377.
(12) Galbally, I. E.; Bentley, S. T.; Meyer, C. P. *Geophys. Res. Lett.* **2000**, *27*, 3841.
(13) Matveev, V.; Peleg, M.; Rosen, D.; Tov-Alper, D. S.; Hebestreit, K.; Stutz, J.; Platt, U.; Blake, D.; Luria, M. *J. Geophys. Res., [Atmos.]* **2001**, *106*, 10375.
(14) Stutz, J.; Ackermann, R.; Fast, J. D.; Barrie, L. *Geophys. Res. Lett.* **2002**, *29*, 1380.
(15) Friess, U.; Hollwedel, J.; König-Langlo, G.; Wagner, T.; Platt, U. *J. Geophys. Res.* **2004**, *109*, D06305.
(16) Hofmeister, F. *Arch. Exp. Pathol. Pharmakol.* **1888**, *24*, 247.
(17) Collins, K. D.; Washabaugh, M. W. *Q. Rev. Biophys.* **1985**, *18*, 323.
(18) Cacace, M. G.; Landau, E. M.; Ramsden, J. J. *Q. Rev. Biophys.* **1997**, *30*, 241.
(19) Zhang, Y.; Cremer, P. S. *Curr. Opin. Chem. Biol.* **2006**, *10*, 658.
(20) Liu, D. F.; Ma, G.; Levering, L. M.; Allen, H. C. *J. Phys. Chem. B* **2004**, *108*, 2252.
(21) Petersen, P. B.; Johnson, J. C.; Knutsen, K. P.; Saykally, R. J. *Chem. Phys. Lett.* **2004**, *397*, 46.
(22) Ghosal, S.; Hemminger, J. C.; Bluhm, H.; Mun, B. S.; Hebenstreit, E. L. D.; Ketteler, G.; Ogletree, D. F.; Requejo, F. G.; Salmeron, M. *Science* **2005**, *307*, 563.
(23) Petersen, P. B.; Saykally, R. J.; Mucha, M.; Jungwirth, P. *J. Phys. Chem. B* **2005**, *109*, 10915.
(24) Onsager, L.; Samaras, N. N. T. *J. Chem. Phys.* **1934**, 528.
(25) Cheng, J.; Vecitis, C. D.; Hoffmann, M. R.; Colussi, A. J. *J. Phys. Chem. B* **2006**, *110*, 25598.
(26) Collins, K. D. *Methods* **2004**, *34*, 300.
(27) Noah-Vanhoucke, J.; Geissler, P. L. *Proc. Natl. Acad. Sci. U.S.A.* **2009**, *106*, 15125.
(28) Pegram, L. M.; Record, M. T. *Proc. Natl. Acad. Sci. U.S.A.* **2006**, *103*, 14278.
(29) Pegram, L. M.; Record, M. T. *J. Phys. Chem. B* **2007**, *111*, 5411.
(30) Ghosal, S.; Brown, M. A.; Bluhm, H.; Krisch, M. J.; Salmeron, M.; Jungwirth, P.; Hemminger, J. C. *J. Phys. Chem. A* **2008**, *112*, 12378.
(31) Krisch, M. J.; D'Auria, R.; Brown, M. A.; Tobias, D. J.; Hemminger, J. C.; Ammann, M.; Starr, D. E.; Bluhm, H. *J. Phys. Chem. C* **2007**, *111*, 13497.
(32) Ostroverkhov, V.; Waychunas, G. A.; Shen, Y. R. *Phys. Rev. Lett.* **2005**, *94*, 046102.

(33) Ji, N.; Ostroverkhov, V.; Chen, C.-Y.; Shen, Y.-R. *J. Am. Chem. Soc.* **2007**, *129*, 10056.
(34) Tian, C. S.; Shen, Y. R. *Chem. Phys. Lett.* **2009**, *470*, 1.
(35) Viswanath, P.; Motschmann, H. *J. Phys. Chem. C* **2007**, *111*, 4484.
(36) Viswanath, P.; Motschmann, H. *J. Phys. Chem. C* **2008**, *112*, 2099.
(37) Chen, X.; Yang, T.; Kataoka, S.; Cremer, P. S. *J. Am. Chem. Soc.* **2007**, *129*, 12272.
(38) Bian, H. T.; Feng, R. R.; Xu, Y. Y.; Guo, Y.; Wang, H. F. *Phys. Chem. Chem. Phys.* **2008**, *10*, 4920.
(39) Petersen, P. B.; Saykally, R. J. *Chem. Phys. Lett.* **2004**, *397*, 51.
(40) Petersen, P. B.; Saykally, R. J. *J. Am. Chem. Soc.* **2005**, *127*, 15446.
(41) Petersen, P. B.; Saykally, R. J. *J. Phys. Chem. B* **2005**, *109*, 7976.
(42) Petersen, P. B.; Saykally, R. J. *J. Phys. Chem. B* **2006**, *110*, 14060.
(43) Otten, D. E.; Petersen, P. B.; Saykally, R. J. *Chem. Phys. Lett.* **2007**, *449*, 261.
(44) Petersen, P. B.; Saykally, R. J. *Chem. Phys. Lett.* **2008**, *458*, 255.
(45) Onorato, R. M.; Otten, D. E.; Saykally, R. J. *Proc. Natl. Acad. Sci. U.S.A.* **2009**, *106*, 15176.
(46) Casson, B. D.; Braun, R.; Bain, C. D. *Faraday Discuss.* **1996**, 209.
(47) Blandamer, M. J.; Fox, M. F. *Chem. Rev.* **1970**, *70*, 59.
(48) Wang, H. F.; Borguet, E.; Eisenthal, K. B. *J. Phys. Chem. B* **1998**, *102*, 4927.
(49) Jungwirth, P.; Tobias, D. J. *J. Phys. Chem. B* **2002**, *106*, 6361.
(50) Jungwirth, P.; Tobias, D. J. *Chem. Rev.* **2006**, *106*, 1259.
(51) Casson, B. D.; Bain, C. D. *Langmuir* **1997**, *13*, 5465.
(52) Renault, A.; Legrand, J. F.; Goldmann, M.; Berge, B. *J. Phys. II* **1993**, *3*, 761.
(53) Legrand, J. F.; Renault, A.; Konovalov, O.; Chevigny, E.; Alsnielsen, J.; Grubel, G.; Berge, B. *Thin Solid Films* **1994**, *248*, 95.
(54) Stanners, C. D.; Du, Q.; Chin, R. P.; Cremer, P.; Somorjai, G. A.; Shen, Y.-R. *Chem. Phys. Lett.* **1995**, *232*, 407.

JP103454R